PHYSICAL REVIEW A **105**, 023520 (2022)

Attosecond measurement via high-order harmonic generation in low-frequency fields

Graham G. Brown,* Dong Hyuk Ko, Chunmei Zhang,* and P. B. Corkum
Department of Physics, University of Ottawa, Ottawa, Canada K1N 6N5
and National Research Council of Canada, Ottawa, Canada K1A 0R6

(Received 4 September 2021; accepted 10 November 2021; published 24 February 2022)

The spectral phase of high-order harmonic and attosecond pulses is typically shaped by the interaction of the recollision electron with the strong field in the continuum. However, the phase of the transition-moment coupling bound and continuum states can be significant in shaping the emitted radiation. It has commonly been assumed that the propagation and recombination steps of the recollision process can be described independently. Here, we investigate the effect that the transition moment has recollision trajectories by incorporating the transition-moment phase into the Lewenstein model of recollision. We then use our model to investigate the all-optical measurement of the transition-moment phase around the Cooper minimum in argon and the spectral minimum due to two-center interference in a diatomic molecular system. Our results indicate that, while all-optical methods are generally sensitive to the transition-moment phase, they are insensitive to the phase shifts due to two-center interference and ionic structure. Thus, we have resolved the apparent discrepancy between studies with conflicting conclusions regarding the sensitivity of all-optical approaches to the transition-moment phase. Our work demonstrates that all-optical measurements focus on photorecombination time delays attributable to electronic structure and dynamics. Our method will allow any laboratory capable of generating attosecond pulses to perform these measurements, even at wavelengths at which the single-photoionization cross section becomes small.

DOI: 10.1103/PhysRevA.105.023520

I. INTRODUCTION

Visible or infrared ultrafast optical technology requires a nonlinear interaction for generating ultrashort pulses and for measuring ultrafast phenomena. Nonlinearity is essential because it allows information to be shared between the frequencies that make up any wave packet. In a laser oscillator, nonlinear optics ensures that there is an exchange of energy between modes that allows them to become locked in phase. For a measurement, nonlinearity is equally important, and the nonlinear process can be, but does not need to be, all optical. The issue that we address in this paper is, Are all-optical approaches [1,2] permitted in attosecond science?

A semiclassical theory of extreme nonlinear optics and recollision was introduced in this journal in 1994 [3]. This theory, known as the Lewenstein model, provided the classical model [4] of recollision with a rigorous quantum-mechanical foundation. Within this theory, the three-step recollision process consists of an electron in the presence of a strong field (1) tunneling into the continuum, (2) being accelerated by the strong field, and (3) recombining into its initial state and emitting an XUV photon. The phase of the emitted radiation is predominantly shaped by the continuum propagation of the ionized electron [5,6] but can be significantly shaped by the phase of the transition moment coupling the initial and continuum states [7–10].

At that time, the important issue was high-order harmonic generation, and so the potential of using extreme nonlinear optics for measurement was not addressed. Yet the formalism introduced in that paper clarifies what has since become a very controversial issue of measurement [8,10], just as it clarified the issue of attosecond pulse generation at the time it was published: whether all-optical approaches are permitted in attosecond science is directly related to how each step of the recollision process is related.

The controversy can be understood by considering the three-step model of high-order harmonic generation, introduced in 1993 [4]. Although not stated at the time, the three steps appear to be independent [11]. Quantitative rescattering [12] (introduced later) made the independence of the steps a formal assumption. If the steps are truly independent, then nonlinear optics can measure only those steps that are optically influenced, and it is the recollision electron trajectory in the continuum that is most easily influenced. Thus, it would seem that nonlinear optics might have little to say about the dynamics of ionization or recombination. This perspective is supported by studies comparing all-optical measurement with photoionization-based attosecond measurement [13] in systems exhibiting a transition-moment phase shift due to two-center interference [8] and a shape resonance [10]. However, this perspective is challenged by recent experimental and theoretical work demonstrating the all-optical measurement of the transition-moment phase around the Cooper minimum in argon [14].

It is not that attosecond dynamics cannot be measured by other nonlinearities. There is little controversy, but much

---

[*] Corresponding authors: graham.brown@uottawa.ca; chunmei.zhang@uottawa.ca

complexity, about attosecond measurements using photoelectron spectroscopy [2,13,15]. This, however, is not merely an academic issue. High harmonics seem to be a universal response of matter when irradiated by an intense field [16,17], and it is important to make attosecond measurements in all these media. If we are confined to photoelectron spectroscopy, attosecond measurements will be possible only in near vacuum.

However, one can easily understand an alternate perspective. The observation of coherent radiation from recollision requires the recolliding electron to return to its initial state [3]. The requirement for recombination to the same initial state acts analogously to phase matching in determining attosecond pulse emission. If the transition moment coupling the initial and continuum states is complex, then phase matching favors components of the continuum electron wave packet appropriately phased with respect to both the initial state and the transition moment to dominate dipole emission. That is, the transition moment affects not only ionization and recombination but continuum propagation as well.

In this paper, we will show how this occurs during recollision and thereby how fully optical measurements of attosecond dynamics can be accomplished. We do this by first extending the Lewenstein model of recollision, the strong-field approximation (SFA) [3], to account for phase shifts in the transition moment between bound and continuum states. We then describe all-optical attosecond measurement [1] and investigate its application in systems with transition-moment phase shifts due to electronic structure [18] and due to ionic structure [8,19]. Our results show that the sensitivity of all-optical measurement to the transition-moment phase shift depends on the origin of the phase shift. In particular, we show all-optical measurement is insensitive to phase shifts arising from ionic structure but is sensitive to phase shifts pertaining to electronic structure and dynamics.

II. THE STRONG-FIELD APPROXIMATION AND ATTOSECOND *In Situ* MEASUREMENT

A. The strong-field approximation with a transition-moment phase

We begin with a single-active-electron atom with ground state $|\psi_0\rangle$ and ionization potential I_p. We then consider recollision driven by a time-dependent strong laser field $E(t)$ polarized along $\hat{z}$ with vector potential $A(t)$. We omit vector notation because all parameters herein are oriented along $\hat{z}$. We define $P(t) = k + A(t)$ as the recollision electron kinetic momentum, where k is the electron canonical momentum. We work within the same assumptions as in [3]: (i) the contribution of all bound states except the ground state can be neglected, (ii) ground-state depletion is neglected, and (iii) the influence of the ionic potential in the continuum is neglected.

Within the SFA, the time-dependent recollision dipole spectrum at time t_r can be expressed as follows [3]:

$$D(t_r) = -i\int dk \int_{-\infty}^{t_r} dt_b d^*(P(t_r)) \times e^{-i[S(k,t_b,t_r)+I_p(t_r-t_b)]}E(t_b)d(P(t_b)), \tag{1}$$

where t_b is the time of ionization, t_r is the time of recombination, $S(k, t_b, t_r)$ is the semiclassical action,

$$S(k, t_b, t_r) = \frac{1}{2}\int_{t_b}^{t_r} [k + A(\tau)]^2 d\tau, \tag{2}$$

and $d(k)$ is the complex transition moment along $\hat{z}$,

$$d(k) = \langle k|\hat{z}|\psi_0\rangle. \tag{3}$$

The total integrand phase is then

$$\Phi_{\text{tot}}(k, t_b, t_r) = S(k, t_b, t_r) + I_p(t_r - t_b) + \Phi[k + A(t_b)] - \Phi[k + A(t_r)], \tag{4}$$

where $I_p(t_r - t_b)$ describes the evolution of the ground-state wave function and $\Phi(k) = \arg[d(k)]$.

Equation (1) is typically solved using a saddle-point approximation [20], wherein the stationary points (i.e., the saddle-point solutions) of the integrand phase in Eq. (4) are used to select the dominant components of the integrand. The integral is then approximated as a weighted summation over the integrand evaluated at the saddle-point solutions. Thus, the stationary-phase analysis is analogous to phase matching, selecting only components of the recollision electron wave packet which are appropriately phased [3].

Within the initial description of the SFA, it is assumed that the integrand phase is predominantly determined by the semiclassical action and the evolution of the ground state. That is, it is assumed that the transition moment varies slowly and can be neglected in the saddle-point analysis. This approximation is applicable in many systems, and the saddle-point solutions provide the link between the quantum-mechanical and semiclassical recollision models [4].

As implied in [3], however, this assumption does not apply to systems with a rapidly varying transition moment. In such systems, the variation of the transition-moment phase can be on the same order as the semiclassical action, and it must be included in the saddle-point analysis. The measurement of the effect that this phase has on the saddle-point solutions is the subject of this paper.

B. Attosecond *in situ* measurement

Optical measurements of recollision are accomplished by perturbing recollision with a weak infrared field. The perturbation modulates recollision trajectories, and these modulations are used to reconstruct recollision dynamics [2]. Since these measurements are performed during the recollision process itself, they are referred to as *in situ* measurement.

Many variations of *in situ* measurement exist [1,2,21,22]. We consider a measurement used to characterize high-order harmonic spectra generated with long driving pulses wherein a copolarized, cophased, and collinear weak second harmonic of the driving field perturbs recollision [1]. The driving and perturbing field vector potentials at time t are given, respectively, as follows:

$$A(t) = A_0 \sin(\omega_0 t), \tag{5}$$

$$A_p(t) = \eta A_0 \sin(2\omega_0 t + \phi), \tag{6}$$

where A_0 is the driving field vector potential amplitude, ω_0 is the driving field frequency, and η and ϕ are the relative amplitude and phase between the driving and perturbing fields. It is assumed that $\eta \ll 1$ and is sufficiently small that the perturbing field does not affect the saddle-point analysis.

In situ measurement was originally described in systems in which the transition-moment phase is slowly varying. Thus, the effect of the perturbing field is included solely within Eq. (2), and the effect of the perturbing field on the transition moment is neglected. With this assumption, the phase shift of the recollision electron induced by perturbation results from the expansion of the semiclassical action to first order in η:

$$\sigma_0(k, t_b, t_r, \phi) = \int_{t_b}^{t_r} [k + A(\tau)]A_p(\tau, \phi)d\tau. \tag{7}$$

Here, however, we are interested in the case where the transition-moment phase is rapidly varying and cannot be neglected. In this case, the total perturbation-induced phase shift is found by expanding the total phase in Eq. (4) to first order in η and is given as follows:

$$\begin{aligned}\sigma(k, t_b, t_r, \phi) = \sigma_0(k, t_b, t_r, \phi) + A_p(t_b, \phi)\Phi'(P(t_b))\\ - A_p(t_r)\Phi'(P(t_r)).\end{aligned} \tag{8}$$

This phase shift is affected by the transition moment in two ways. First, the transition moment affects the saddle-point solutions and thus directly affects the semiclassical action $\sigma_0(k, t_b, t_r, \phi)$. Second, the measurement is affected by the influence of the perturbing field on the transition moment.

With Eqs. (5)–(8), the perturbation-induced phase shift can be factored into rapidly and slowly varying components, $\Sigma(k, t_b, t_r)$ and $\cos[\phi - \theta(k, t_b, t_r)]$, respectively, as follows [1]:

$$\begin{aligned}\sigma(k, t_b, t_r, \phi) &= \sigma_c(k, t_b, t_r)\sin(\phi) + \sigma_s(k, t_b, t_r)\cos(\phi)\\ &= \Sigma(k, t_b, t_r)\cos[\phi - \theta(k, t_b, t_r)],\end{aligned} \tag{9}$$

where

$$\Sigma(k, t_b, t_r) = \sqrt{\sigma_c^2(k, t_b, t_r) + \sigma_s^2(k, t_b, t_r)}, \tag{10}$$

$$\theta(k, t_b, t_r) = \arctan\left(\frac{\sigma_c(k, t_b, t_r)}{\sigma_s(k, t_b, t_r)}\right). \tag{11}$$

We now consider the perturbed dipole emission from two adjacent half cycles, $D_L(t)$ and $D_R(t)$, of the driving field, which we label as left (L) and right (R), respectively. Symmetry requires that the unperturbed dipole emissions from the left and right half cycles exhibit a π-phase difference and that the perturbation-induced phase shift in each half cycle is equal but opposite in sign. With this, the superposition of the dipole emission from the left and right half cycles $D(t_r, \phi)$ satisfies the following:

$$D(t_r, \phi) \propto \int dk \int_{-\infty}^{t_r} dt_b \sigma(k, t_b, t_r, \phi) D_L(k, t_b, t_r). \tag{12}$$

The dipole spectrum at even harmonic $2N$ (integer N) is found through the Fourier transform of Eq. (12) at frequency $2N\omega_0$. We define $\Phi_{\mathrm{tot}}(t) = -i\ln[\Sigma(k, t_b, t_r) + D_L(t)]$, such that

$$\begin{aligned}\tilde{D}(2N\omega_0, \phi) \propto \int dk \int_{-\infty}^{\infty} dt_r \int_{-\infty}^{t_r} e^{i\Phi_{\mathrm{tot}}(t_r)}\\ \times \cos[\phi - \theta(k, t_b, t_r)]e^{2iN\omega_0 t_r}.\end{aligned} \tag{13}$$

After finding the unperturbed saddle-point solutions, the variation of the $2N$th even-harmonic intensity with respect to the relative phase ϕ is given as

$$|\tilde{D}(2N\omega_0, \phi)|^2 \propto \cos^2[\phi - \theta(k, t_b, t_r)]. \tag{14}$$

Experimentally, the relative phase which maximizes the even-harmonic signal is recorded while varying the relative phase between the driving and perturbing fields. From Eq. (14), the even-harmonic signal is maximized when $\phi = \theta(k, t_b, t_r)$. Thus, we call $\theta(k, t_b, t_r)$ the maximizing phase. Since the maximizing phase has an analytic expression, the measured maximizing phase can be related directly to the recollision dynamics for each even harmonic. Thus, the feasibility of *in situ* measurement to measure the transition-moment phase in the subsequent section will be determined through the maximizing phase $\theta(k, t_b, t_r)$.

III. *In Situ* MEASUREMENT AND THE TRANSITION-MOMENT PHASE

We are now ready to describe *in situ* measurement in systems exhibiting a transition-moment phase shift. We first consider the case of a transition-moment phase shift due to electronic structure, using the Cooper minimum in argon as an example [18]. We then consider the measurement of recollision in a diatomic molecule [8,19], which exhibits a π-phase jump in its transition moment due to two-center interference. We will demonstrate that *in situ* measurement is generally sensitive to the transition-moment phase but is insensitive to phase shifts arising from ionic structure.

For consistency, all our results are calculated using a sinusoidal driving field with a wavelength of 1.8 μm and peak intensity of 1×10^{14} W/cm^2 and a perturbing copolarized second-order harmonic field with a relative intensity of 10^{-4}.

A. Cooper minimum in argon

We consider an atomic system with an ionization potential of 15.8 eV with a transition-moment cross section and phase as depicted in Fig. 1. A spectral minimum and π-phase shift are observed near 52 eV. We choose this model as it provides a simple description of the transition-moment phase in argon including both s- and d-wave continuum channels [7]. We incorporate the transition-moment phase $\Phi(k)$ at momentum k into the saddle-point analysis of the SFA by using the following modified saddle-point equations to find the dipole moment in the time domain:

$$0 = \int_{t_b}^{t_r} P(\tau)d\tau - \Phi'(P(t_r)) + \Phi'(P(t_b)), \tag{15}$$

$$0 = \frac{P^2(t_b)}{2} + I_p + E(t_b)\Phi'(P(t_b)), \tag{16}$$

We numerically solve Eqs. (15) and (16) in the time domain for the saddle-point solutions with the transition-moment

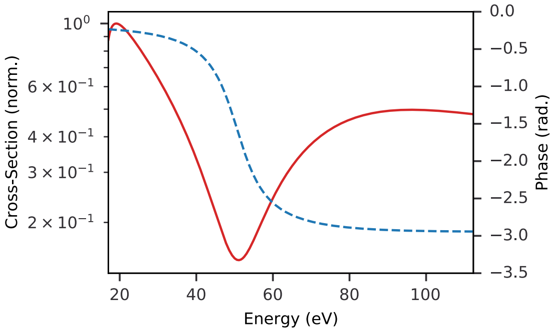

FIG. 1. The recombination cross section (solid red line) and phase (dashed blue line) for the model argon atom are plotted on the left and right axes, respectively. A spectral minimum and π-phase shift occur near 52 eV.

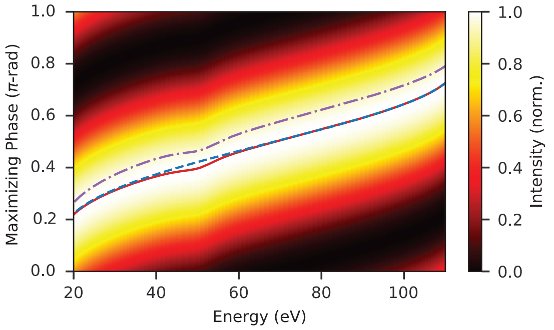

FIG. 3. The spectrogram showing the variation of the even-harmonic intensity in an *in situ* measurement of the model argon atom with respect to the relative phase between the driving and perturbing fields. The overlaid solid red and dashed blue lines show the maximizing phase for the model argon and reference atoms, respectively. The overlaid purple dash-dotted line depicts the scaled excursion time as shown in Fig. 2. The driving field intensity and wavelength are 1×10^{14} W/cm^{-2}.

phase in Fig. 1. Figure 2(a) depicts the trajectory excursion time as a function of the emitted photon energy from the system including the transition-moment phase (solid red line) and a reference equivalent system without the transition moment phase (dashed blue line). The excursion time for the system with the transition-moment phase shift deviates from the reference system around 52 eV due to the transition-moment phase shift. This difference is depicted in Fig. 2(b) along the left axis (solid red line) and is largest (−145 as) near 50 eV.

Within the modified saddle-point equations, the gradient of the transition-moment phase acts equivalently to a spatial offset. The return condition in Eq. (15) is offset by the difference in the transition-moment phase at the times of ionization and recombination. In Eq. (16), the condition for energy conservation during the ionization step is shifted in energy analogously to a dipole interaction between the driving electric field and the transition-moment phase gradient. Thus, we expect the relative positions of ionization and recombination to depend on the gradient of the transition-moment phase.

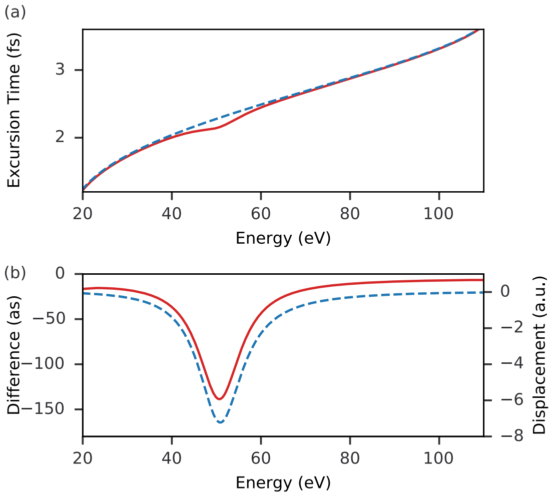

FIG. 2. (a) The short-trajectory excursion times as a function of emitted photon energy calculated with (solid red line) and without (dashed blue line) the transition-moment phase from Fig. 1 in Eqs. (15) and (16). (b) The difference in excursion time between the systems with and without the transition-moment phase from the excursion times presented in (a) (solid red line) is plotted on the left axis. The difference in the positions of ionization and recombination for the trajectories leading to photon emission at a given energy (dashed blue line) is plotted on the right axis. The sinusoidal driving field intensity and wavelength are 1×10^{14} W/cm^{-2}.

Figure 2(b) shows the difference between the positions of ionization and recombination Δx along the right axis (dashed blue line). The structure of Δx reflects the structure of the change in excursion time. In argon, the Cooper minimum results from the nodal structure of the ground-state wave function [18], wherein the radial ground-state wave function exhibits a tightly bound inner lobe and a larger outer lobe with a radial extent of ~10 a.u. Below the spectral minimum, dipole emission from the outer lobe dominates dipole emission. At the spectral minimum, the dipole emission from these lobes cancels. Above the spectral minimum, the lobe which dominates dipole emission changes, resulting in a shift in the position of photon emission. Thus, we interpret the variation in Fig. 2(b) as a consequence of the structure of the ground-state wave function.

We are now ready to consider an *in situ* measurement. We use Eqs. (8) and (11) to calculate the phase $\theta(k, t_b, t_r)$ which maximizes the even-harmonic signal and Eq. (14) to calculate the variation of the even-harmonic intensity with the relative phase between the driving and perturbing fields. We perform the same calculation for an equivalent system without a transition-moment phase to use as a reference.

The resultant spectrogram depicting the normalized variation of the even-harmonic intensity with the relative phase between the driving and perturbing fields is shown in Fig. 3. The overlaid solid red line depicts the maximizing phase $\theta(k, t_b, t_r)$ calculated from the model argon atom, while the dashed blue line shows the same result for the reference atom. A clear deviation from the reference around 52 eV is observed in the result that includes the transition-moment phase. Above and below the resonance, the two results agree. The trajectory excursion time from our model argon atom (dot-dashed purple line) agrees with the maximizing phase, indicating that *in situ* measurement is sensitive to the transition-moment phase. This result agrees with recent experimental and theoretical work [14] reporting the *in situ* measurement of photorecombination time delays around the Cooper minimum in argon.

As mentioned previously, however, it is well accepted within the attosecond science community that *in situ* measurement is incapable of measuring the transition-moment phase [8]. It has been argued that the perturbing field does not significantly affect the transition moment enough to have a measurable effect. However, as demonstrated in Sec. II A and Fig. 2, the perturbing field does not need to affect the transition moment. Attosecond pulse generation occurs when the continuum electron wave packet overlaps with the ground state, resulting in an oscillating dipole which returns the system to its initial state. The components of the recollision electron wave packet which dominate dipole emission are determined through phase-matching conditions dictated by the strong driving field and atomic or molecular system. In systems with a real, or slowly varying, transition moment, the phase-matching conditions are determined by the strong driving field and result in the well-known attochirp.

In systems with a rapidly varying transition-moment phase, however, the variation of the transition moment phase can be comparable to that of the semiclassical action. In such cases, the transition-moment phase must be taken into account in the SFA saddle-point analysis, as in Sec. II A. The transition-moment phase then modifies the phase-matching conditions and thus which recollision trajectories dominate dipole emission. These trajectories are measurable, and this measurement does not require the perturbing field to affect the transition moment.

B. Ionic structure

We now address the apparent discrepancy between the recent experimental and theoretical study of an *in situ* measurement in argon [14] and the study which demonstrated attosecond *in situ* measurement is insensitive to the transition-moment phase associated with two-center interference in diatomic molecular systems [8]. The two-center study compared attosecond *in situ* measurement with a conventional photoionization-based attosecond measurement technique [13] and found that, while the conventional measurement is sensitive to the transition-moment phase, the effect of the phase shift was completely absent from the *in situ* measurement. Here, we show that our analysis is consistent with that study. The insensitivity of *in situ* measurement to two-center interference is a characteristic of phase shifts arising from ionic structure.

There are several methods for calculating recollision processes in diatomic molecules using the SFA. We use the formalism presented in [23] due to the agreement of the dipole phase with numerical time-dependent Schrödinger equation simulations. For simplicity, we consider a one-dimensional diatomic molecule with atomic centers located at $x = \pm R/2$, where R is the internuclear separation. We label the atomic centers of ionization and recombination as $\alpha, \beta = 1, 2$, respectively, such that the positions of ionization and recombination are $(-1)^{\gamma} R/2$, with $\gamma = \alpha, \beta$. Accordingly, we label the parameters for each trajectory with the subscript $\alpha\beta$. Our analysis can easily be extended to more complex systems.

We describe the ground state $\psi(x)$ using a linear combination of atomic orbitals centered at each atomic center. Recombination and ionization from atom α at momentum k and time t are described by the following matrix elements:

$$d_{\mathrm{rec}}(k) = \mathcal{R}(k)(e^{ikR/2} + e^{-ikR/2}), \tag{17}$$

$$d_{\mathrm{ion}}(k, t) = \mathcal{J}_1(k, t)e^{ikR/2} + \mathcal{J}_2(k, t)e^{-ikR/2}, \tag{18}$$

where $\mathcal{R}(k)$ and $\mathcal{J}_{\alpha}(k, t)$ denote the recombination and ionization matrix elements for the atomic orbital which makes up the ground state. With these, the recollision dipole spectrum is represented as the sum of four terms, corresponding to each $\alpha\beta$ trajectory:

$$\tilde{D}(\Omega) = \sum_{\alpha,\beta=1}^{2} \int dk \int_{-\infty}^{\infty} dt_r \int_{-\infty}^{t_r} dt_b \mathcal{R}(P(t_r))\mathcal{J}_{\alpha}(P(t_b), t_b) \times e^{-i[S(k,t_b,t_r)-\Omega t_r+\Phi_{\alpha}(P(t_b))-\Phi_{\beta}(P(t_r))]}, \tag{19}$$

where

$$\Phi_{\gamma}(k) = (-1)^{\gamma} k \frac{R}{2} \tag{20}$$

acts as an effective transition-moment phase for the $\alpha\beta$ trajectory. From Eq. (20), the gradient of the transition-moment phase $\Phi'_{\gamma}(k) = (-1)^{\gamma} R/2$ is a constant.

The changes to the saddle-point solutions from a simple atomic system due to the transition-moment phase in Eq. (20) are small. As in [23], we find the first-order Taylor expansion of the saddle-point equations in the frequency domain to first order with respect to R using Eq. (20). We perform this expansion about the saddle-point solutions for a system without a transition-moment phase, $\bar{k}$, $\bar{t}_b$, and $\bar{t}_r$, which we label as the zeroth-order solutions. This results in the following corrections to the saddle-point solutions from the zeroth-order solution for each $\alpha\beta$ trajectory [23]:

$$\Delta k^{(1)}_{\alpha\beta} = 0, \tag{21}$$

$$\Delta t^{(1)}_{b,\alpha} = \frac{(-1)^{\alpha} R}{2[\bar{k} + A(\bar{t}_b)]}, \tag{22}$$

$$\Delta t^{(1)}_{r,\beta} = \frac{(-1)^{\beta} R}{2[\bar{k} + A(\bar{t}_r)]}. \tag{23}$$

As shown in [23], the dipole moment in Eq. (19) can be expanded to first order in R using these saddle-point corrections. The first-order recombination transition-moment cross section and phase calculated with this model are shown in Fig. 4. Although it appears like the transition moment depicted in Fig. 1 for the model argon atom, the origin of the spectral minimum in each case differs. While the Cooper minimum is a result of the structure of the ground-state wave function, the spectral minimum here results from the interference of the four possible $\alpha\beta$ trajectories.

From Eqs. (21)–(23), it is apparent that the individual trajectories do not reflect the spectral structure of the transition-moment phase. This is demonstrated in Fig. 5, which shows the recombination times for trajectories with $\beta = 1, 2$ (bottom red and top blue solid lines, respectively)

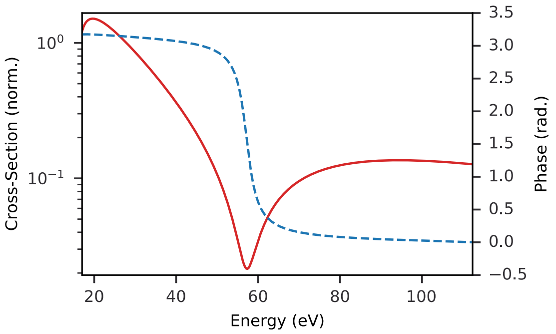

FIG. 4. The recombination cross section and phase for a one-dimensional diatomic molecule with an internuclear separation of 1.8 a.u. and ionization potential of 15.8 eV calculated using Eqs. (21)–(23), the first-order approximation given in [23], and a sinusoidal driving field with a wavelength of 1.8 μm and peak intensity of 1×10^{14} W/cm^2.

and the recombination time for the reference atomic system (dashed green line). The correction to the recombination time corresponds to the time required for an electron of kinetic momentum $P(\bar{t}_r)$ to travel a distance of $(-1)^\beta R/2$ and varies adiabatically with the electron kinetic energy.

We now consider an *in situ* measurement in a two-center system. Since $|\Delta t^{(1)}_{r,\beta}|/\bar{t}_r \ll 1$, we expand Eq. (8) to first order in $\Delta t^{(1)}_{r,\beta}$ for each $\alpha\beta$ trajectory. A similar analysis can be done while accounting for the correction to the ionization time, but we omit it for brevity. Given that the recollision phase is predominantly shaped by continuum propagation and recombination, this omission does not affect our results or conclusions. To first order in $\Delta t^{(1)}_{r,\beta}$, the perturbation-induced phase shift for trajectories recombining to atomic center β can be approximated as follows:

$$\sigma_\beta(k,t_b,t_r,\phi) \approx \sigma_0(\bar{k},\bar{t}_b,\bar{t}_r,\phi) - A_p(\bar{t}_r,\phi)\Phi'_\beta(P(\bar{t}_r)) + \left(E_p(\bar{t}_r,\phi)\Phi'(P(\bar{t}_r)) + \frac{\partial\sigma_0}{\partial t_r}\bigg|_{\bar{k},\bar{t}_b,\bar{t}_r} + E(\bar{t}_r)A_p(\bar{t}_r,\phi)\Phi''_\beta(P(\bar{t}_r))\right)\Delta t^{(1)}_{r,\beta}, \quad (24)$$

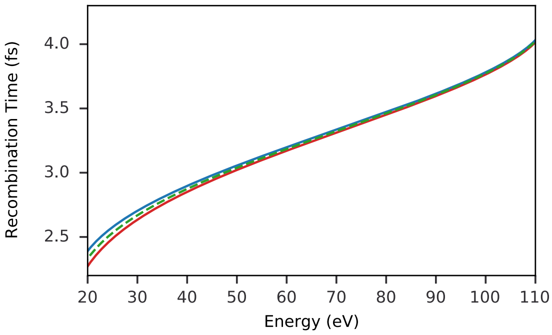

FIG. 5. The recombination times for trajectories recombining to the left (bottom red line) and right (top blue line) atomic centers in a diatomic molecule with internuclear separation $R = 1.8$ a.u and an ionization potential of 15.8 eV are shown. The recombination times in a reference atom with an equivalent ionization potential are shown by the dashed green line. A sinusoidal driving field with a wavelength of 1.8μ and peak intensity of 1×10^{14} W/cm^2 is used.

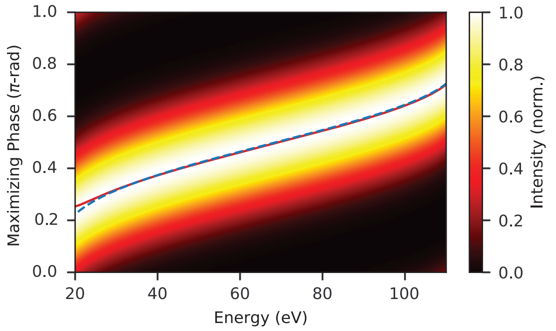

FIG. 6. The spectrogram showing the variation of the even-harmonic intensity in an *in situ* measurement in the two-center system with respect to the relative phase between the driving and perturbing fields. The overlaid solid red and dashed blue lines show the maximizing phase for the diatomic molecule and reference atom, respectively. The driving field intensity and wavelength are 1×10^{14} W/cm^{-2}.

where we have retained solely terms which include the perturbing field. Within this first-order approximation, the influence of the perturbing field on the transition moment exactly cancels the change in $\sigma_0(k,t_b,t_r,\phi)$ due to $\Delta t^{(1)}_{r,\beta}$ since

$$\frac{\partial\sigma_0}{\partial t_r}\Delta t^{(1)}_{r,\beta} = A_p(\bar{t}_r,\phi)\Phi'_\beta(P(\bar{t}_r)). \quad (25)$$

Further, the phase $\Phi_\beta(k)$ varies linearly with respect to momentum, and therefore, $\Phi''_\beta(k) = 0$. The total perturbation-induced phase shift is then given as follows:

$$\sigma_\beta(k,t_b,t_r,\phi) = \sigma_0(\bar{k},\bar{t}_b,\bar{t}_r,\phi) + \frac{E_p(\bar{t}_r,\phi)}{\bar{k}+A(\bar{t}_r)}R^2. \quad (26)$$

The effective perturbation-induced phase shift is equal to the sum of that in a system without a transition-moment phase and a term proportional to the square of the distance of the displaced recombination atomic center to the origin. Thus, all trajectories exhibit the same perturbation-induced phase shift. Further, the change in the perturbation-induced phase shift is small since $\omega_0 \ll 1$. Therefore, the results of an *in situ* measurement in a two-center system and reference atomic system will exhibit negligible differences. This is in contrast to the study of the Cooper minimum in argon, wherein the transition-moment phase is not a linear function of momentum and the large variation of the phase shift within a single recollision trajectory necessitates higher-order descriptions of the measurement.

This is confirmed in Fig. 6, which depicts a spectrogram of the variation of the even-harmonic intensity with the relative phase between the driving and perturbing fields. The overlaid solid red and dashed blue lines depict the maximizing phase for the two-center and an equivalent reference atomic system. The results for the diatomic molecule and reference atomic system are nearly identical, except at low energies, and the structure of the phase jump in Fig. 4 is completely absent. The difference in the maximizing phase for the two-center and reference atomic systems is shown in Fig. 7. Like the change in recombination time due to molecular structure, the difference in maximizing phase between the two-center system

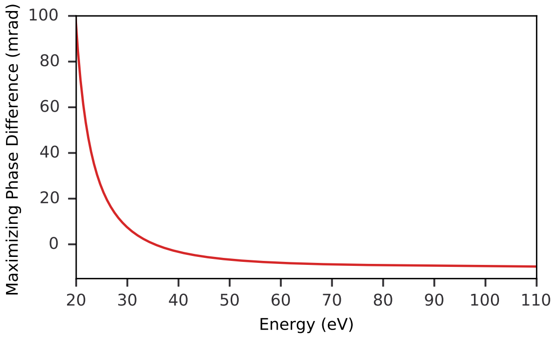

FIG. 7. The difference in the maximizing phase between the diatomic molecule and reference atomic systems from the simulated *in situ* measurement in Fig. 6.

and reference atom is largest at low energies and decreases monotonically with energy.

This result implies the nature of the transition-moment phase is critical in determining the sensitivity of *in situ* measurement to recombination dynamics. We expect that we can use differences between a conventional photoionization-based streaking experiment and an *in situ* measurement to isolate spectral features of attosecond pulses due to ionic and electronic structure and dynamics.

IV. CONCLUSION

The sensitivity of attosecond *in situ* measurement to transition-moment phase shifts is explained by how the transition-moment phase affects recollision trajectories. If the transition moment is real or its phase varies sufficiently slowly, then its effect on recollision trajectories is negligible, and the semiclassical action dictates the phase-matching conditions. If, however, the transition moment is complex and rapidly varying, its phase can be as important in determining the stationary points as the semiclassical action. Since the ground-state wave function is negligibly varied, phase matching favors components of the recollision wave packet with a spectral phase that complements the transition-moment phase.

Our results demonstrate that the nature of the transition-moment phase determines its effect on recollision trajectories and thereby the sensitivity of *in situ* measurement to such phase shifts. In particular, *in situ* measurement is sensitive to the transition-moment phase but is insensitive to phase shifts due to two-center interference. Thus, we explained the apparent discrepancy between recent experiments reporting photorecombination time-delay measurements using *in situ* techniques in argon [12] and studies which showed these techniques are insensitive to the phase jump from two-center interference. Although we investigated recollision in a diatomic molecule, our results are easily extended to more complex molecular systems.

The all-optical measurements of photorecombination time delays offer a new direction for attosecond measurement without obfuscation from ionic structural effects and can be performed in any laboratory capable of generating high-order harmonic radiation. Such measurements can be used to characterize multielectron interaction [24–26], electronic structure [14,27], and strong-field-driven electron dynamics.

Further, the relationship between photorecombination time delays and electronic structure suggests a form of tomography [28,29] wherein electronic structure is inferred from all-optical measurements. Finally, by combining *in situ* measurement with methods such as the attosecond streak camera or reconstruction of attosecond bursts by two-photon transitions, ionic and electronic effects on the phase of attosecond and high-order harmonic pulses can be isolated.

ACKNOWLEDGMENTS

This research was supported by the U.S. Air Force Office of Scientific Research (Award No. FA9550-16-1-0109) with contributions from the Canada Foundation for Innovation, the Canada Research Chairs program, Canada's Natural Sciences and Engineering Research Council, and the National Research Council of Canada.

---

[1] N. Dudovich, O. Smirnova, J. Levesque, Y. Mairesse, M. Y. Ivanov, D. M. Villeneuve, and P. B. Corkum, Measuring and controlling the birth of attosecond xuv pulses, Nat. Phys. **2**, 781 (2006).

[2] K. T. Kim, D. M. Villeneuve, and P. B. Corkum, Manipulating quantum paths for novel attosecond measurement methods, Nat. Photon. **8**, 187 (2014).

[3] M. Lewenstein, P. Balcou, M. Y. Ivanov, A. L'Huillier, and P. B. Corkum, Theory of high-harmonic generation by low-frequency laser fields, Phys. Rev. A **49**, 2117 (1994).

[4] P. B. Corkum, Plasma Perspective on Strong Field Multiphoton Ionization, Phys. Rev. Lett. **71**, 1994 (1993).

[5] K. Varjú II, Y. Mairesse, B. Carré, M. B. Gaarde, P. Johnsson, S. Kazamias, R. López-Martens, J. Mauritsson, K. J. Schafer, P. Balcou, A. L'Huillier, and P. Salières, Frequency chirp of harmonic and attosecond pulses, J. Mod. Opt. **52**, 379 (2005).

[6] M. Lewenstein, P. Salières, and A. L'Huillier, Phase of the atomic polarization in high-order harmonic generation, Phys. Rev. A **52**, 4747 (1995).

[7] S. B. Schoun, R. Chirla, J. Wheeler, C. Roedig, P. Agostini, L. F. DiMauro, K. J. Schafer, and M. B. Gaarde, Attosecond Pulse Shaping around a Cooper Minimum, Phys. Rev. Lett. **112**, 153001 (2014).

[8] M. Spanner, J. B. Bertrand, and D. M. Villeneuve, In situ attosecond pulse characterization techniques to measure the electromagnetic phase, Phys. Rev. A **94**, 023825 (2016).

[9] A. D. Shiner, B. E. Schmidt, C. Trallero-Herrero, H. J. Wörner, S. Patchkovskii, P. B. Corkum, J.-C. Kieffer, F. Légaré, and D. M. Villeneuve, Probing collective multi-electron dynamics in xenon with high-harmonic spectroscopy, Nat. Phys. **7**, 464 (2011).

[10] G. Orenstein, O. Pedatzur, A. J. Uzan, B. D. Bruner, Y. Mairesse, and N. Dudovich, Isolating strong-field dynamics in molecular systems, Phys. Rev. A **95**, 051401(R) (2017).

[11] A.-T. Le, T. Morishita, and C. D. Lin, Extraction of the species-dependent dipole amplitude and phase from high-order harmonic spectra in rare-gas atoms, Phys. Rev. A **78**, 023814 (2008).

[12] A.-T. Le, R. R. Lucchese, S. Tonzani, T. Morishita, and C. D. Lin, Quantitative rescattering theory for high-order harmonic generation from molecules, Phys. Rev. A **80**, 013401 (2009).

[13] P. M. Paul, E. S. Toma, P. Breger, G. Mullot, F. Augé, P. Balcou, H. G. Muller, and P. Agostini, Observation of a train of attosecond pulses from high harmonic generation, Science **292**, 1689 (2001).

[14] C. Zhang, G. G. Brown, D. H. Ko, and P. B. Corkum, Optical measurement of photorecombination time delays, arXiv:2104.00844.

[15] J. Itatani, F. Quéré, G. L. Yudin, M. Y. Ivanov, F. Krausz, and P. B. Corkum, Attosecond Streak Camera, Phys. Rev. Lett. **88**, 173903 (2002).

[16] G. Vampa, C. R. McDonald, G. Orlando, P. B. Corkum, and T. Brabec, Semiclassical analysis of high harmonic generation in bulk crystals, Phys. Rev. B **91**, 064302 (2015).

[17] T. T. Luu, Z. Yin, A. Jain, T. Gaumnitz, Y. Pertot, J. Ma, and H. J. Wörner, Extreme–ultraviolet high–harmonic generation in liquids, Nat. Commun. **9**, 3723 (2018).

[18] J. W. Cooper, Photoionization from outer atomic subshells. A model study, Phys. Rev. **128**, 681 (1962).

[19] C. Vozzi, F. Calegari, E. Benedetti, J.-P. Caumes, G. Sansone, S. Stagira, M. Nisoli, R. Torres, E. Heesel, N. Kajumba, J. P. Marangos, C. Altucci, and R. Velotta, Controlling Two-Center Interference in Molecular High Harmonic Generation, Phys. Rev. Lett. **95**, 153902 (2005).

[20] A. Nayak *et al.*, Saddle point approaches in strong field physics and generation of attosecond pulses, Phys. Rep. **833**, 1 (2019).

[21] K. T. Kim, C. Zhang, A. D. Shiner, S. E. Kirkwood, E. Frumker, G. Gariepy, A. Naumov, D. M. Villeneuve, and P. B. Corkum, Manipulation of quantum paths for space–time characterization of attosecond pulses, Nat. Phys. **9**, 159 (2013).

[22] D. H. Ko, G. G. Brown, C. Zhang, and P. B. Corkum, Near-field imaging of dipole emission modulated by an optical grating, Optica **8**, 1632 (2021).

[23] M. Labeye, F. Risoud, C. Lévêque, J. Caillat, A. Maquet, T. Shaaran, P. Salières, and R. Taïeb, Dynamical distortions of structural signatures in molecular high-order harmonic spectroscopy, Phys. Rev. A **99**, 013412 (2019).

[24] G. G. Brown, D. H. Ko, C. Zhang, and P. B. Corkum, Characterizing Fano resonances during recollision, arXiv:2010.04834.

[25] S. Pabst and R. Santra, Strong-Field Many-Body Physics and the Giant Enhancement in the High-Harmonic Spectrum of Xenon, Phys. Rev. Lett. **111**, 233005 (2013).

[26] G. G. Brown, D. H. Ko, C. Zhang, and P. B. Corkum, Characterizing multielectron dynamics during recollision, arXiv:2010.06165.

[27] S. L. Molodtsov, S. V. Halilov, V. D. P. Servedio, W. Schneider, S. Danzenbächer, J. J. Hinarejos, M. Richter, and C. Laubschat, Cooper Minima in the Photoemission Spectra of Solids, Phys. Rev. Lett. **85**, 4184 (2000).

[28] J. Itatani, J. Levesque, D. Zeidler, H. Niikura, H. Pépin, J. C. Kieffer, P. B. Corkum, and D. M. Villeneuve, Tomographic imaging of molecular orbitals, Nature (London) **432**, 867 (2004).

[29] J. B. Bertrand, H. J. Wörner, P. Salières, D. M. Villeneuve, and P. B. Corkum, Linked attosecond phase interferometry for molecular frame measurements, Nat. Phys. **9**, 174 (2013).